arXiv:1403.6642v1 [cond-mat.stat-mech] 26 Mar 2014

Escape Dynamics of Many Hard Disks

Tooru Taniguchi, Hiroki Murata and Shin-ichi Sawada
School of Science and Technology, Kwansei Gakuin University, 2-1 Gakuen, Sanda city, Japan
(Dated: March 27, 2014)

Many-particle effects in escapes of hard disks from a square box via a hole are discussed in a viewpoint of dynamical systems. Starting from N disks in the box at the initial time, we calculate the probability $P_n(t)$ for at least n disks to remain inside the box at time t for $n = 1, 2, \cdots, N$. At early times the probabilities $P_n(t)$, $n = 2, 3, \cdots, N-1$ are described by superpositions of exponential decay functions. On the other hand, after a long time the probability $P_n(t)$ decays in power $\sim t^{-2n}$ for $n \neq 1$, in contrast to the fact that it decays in a different power $\sim t^{-n}$ for the case without any disk-disk collision. Chaotic and non-chaotic properties of the escape systems are discussed by the dynamics of finite time largest Lyapunov exponents, whose decay properties are related with those of the probability $P_n(t)$.

PACS numbers: 05.60.Cd, 05.45.Jn, 45.50.Jf

I. INTRODUCTION

The escape of materials from a finite area is known as an essential concept to understand many physical features in a variety of natural phenomena. It describes a wide scale of physical phenomena from a microscopic scale (e.g. α decay of nuclei [1, 2] and light emissions from molecules [3–5]) to a macroscopic one (e.g. ejections or evaporations of stars in cosmology [6, 7]). It also plays an important role to analyze properties of materials, for example, by means of particle escapes from a quantum dot [8–10] or from an optical potential trap [11–13], escape basins of magnetic field lines in plasma [14, 15], and transition of states in chemical reactions (as an escape of excited chemical species from a reactant region) [16–18], etc. The concept of escape is also used to calculate transport coefficients in chaotic dynamical systems [19–21], and as a mechanism to produce electric currents as an escape of electrons from a particle reservoir [22–24]. Escapes occur when particles reach a specific region like a hole, so that they are related to the first passage time problem and the recurrence problem [25–27]. In escape phenomena, states of materials leave their initial ones with a decay, whose kind of features also appear in the Loschmidt echo and fidelity decay [28, 29].

Escape phenomena are characterized by various quantities, such as the survival probability [30–32, 34–38] as the probability for a particle to remain in the initially confined finite area, the escape time [27, 39, 40] as the time period for a particle to stay in the finite area, and a velocity when a particle escapes from the finite area [37],etc. These quantities decay in time as a feature of escape phenomena in which the materials continue escaping from the initially confined area. Many works have already done to clarify their decay properties in escapes of a single particle by using dynamical theories. It is conjectured, for example, that the survival probability decays exponentially in time for chaotic systems based on an ergodic argument, while it decays in power for non-chaotic systems [30]. This conjecture led to further dynamical studies of escape phenomena, clarifying effects of a finite size of holes [32, 39], weakness of chaos [27], specific orbits causing a power decay [33, 34], etc.

The principal aim of this paper is to discuss many-particle effects in dynamical properties of escape phenomena. As a system consisting of many particles, we use many hard disks in a square box, which have been widely used to investigate statistical and dynamical properties [41–43]. At the corner of the box we put a hole where hard disks escape from the box. To discuss escape properties of N disks from the square box via the hole, we introduce the survival probability $P_n(t)$ for n disks to remain inside the box at time t ($n = 1, 2, \cdots, N$). We show that at early times decays of the survival probabilities $P_n(t)$, $n = 2, 3, \cdots, N-1$ are well-described by superpositions of exponential functions. It is also shown that after a long time the survival probability $P_n(t)$ decays in power $\sim t^{-2n}$, while it decays in different power $\sim t^{-n}$ for the case without any disk-disk collision, for $n = 2, 3, \cdots$. This means qualitative changes in decays of survival probabilities by existence of disk-disk collisions and the disk number n, implying that we can get information on particle-particle interactions and the number of non-escape particles from their decay behaviors. We also discuss dynamical properties of escape systems by using the finite time largest Lyapunov exponent (FTLLE) $\lambda(t)$ [44, 45], which is introduced as an exponential rate of expansion or contraction of an infinitesimally small initial error at a finite time t. The FTLLE converges to the well-known largest Lyapunov exponent in the long time limit, whose positivity means dynamics of the system to be chaotic. We compare quantitatively decay properties of the survival probability $P_n(t)$ and the corresponding FTLLE $\lambda(t)$, and clarify roles of chaotic or non-chaotic dynamics in escape phenomena of many hard disks. Dependences of the survival probabilities and the FTLLEs on the system length and the hole size, etc., are also discussed as scaling properties.

The outline of this paper is as follows. In Sec. II we introduce our model consisting of many hard disks in a square box with a hole, and discuss exponential and power decays of survival probabilities of this many-

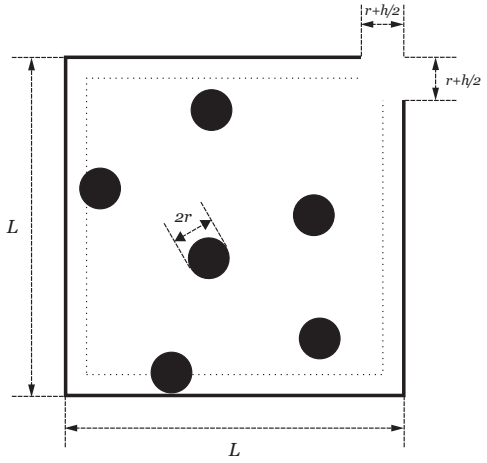

FIG. 1: Many hard disks with the radius r in a square box with length L of each side. The box has a hole with each length $r + (h/2)$ of both the sides from a corner of the box. The dotted lines in inner sides of the box are for positions of the center of disks closest to walls of the box.

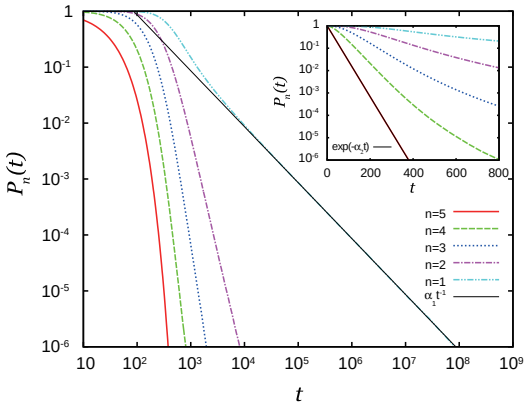

FIG. 2: (Color online) The n-particle survival probabilities $P_n(t)$ of a 5-disk system as functions of time t for $n = 5$ (the solid line), 4 (the dashed line), 3 (the dotted line), 2 (the dash-dotted line), 1 (the dash-double-dotted line). The main figure is for graphs of $P_n(t)$ on log-log plots with a straight shin line for a fitting function $\alpha_1 t^{-1}$ to $P_1(t)$ with the fitting parameters α_1. The inset is for graphs of $P_n(t)$ on linear-log plots with a straight shin line for a fitting function $\exp(-\alpha_2 t)$ to $P_5(t)$ with the fitting parameter α_2.

particle system. In Sec. III we discuss decay properties of FTLLEs in escape systems of many hard disks, and investigate connections between properties of the survival probabilities and the FTLLEs. Finally, we give conclusion and remarks on the contents of this paper in Sec. IV.

II. ESCAPE PROPERTIES OF MANY-HARD-DISK SYSTEMS

A. Many hard disks in a square box with a hole

We consider the system consisting of many hard disks inside a square box with a hole. Here, the mass and the radius of the disks are m and r, respectively, and the length of each side of the box is L, and a hole in the box is put as the region of the length $r + (h/2)$ in both the sides from a single corner of the box, as shown in Fig. 1 as a schematic illustration. Here, the length $h/2$ is the effective length of each side of the hole, where centers of disks can reach. In this system, each disk moves with a velocity, then collides elastically with other disks or walls, or leaves the box via the hole. We assume that any disk does not enter into the box via the hole from its outside, and any disk is removed from the box when it reaches the hole. As an important system parameter we use the particle density $\rho \equiv N\pi r^2/L^2$ of the system at the initial time $t = 0$.

B. Survival probabilities of many-hard-disk systems

To characterize escape behaviors of N disks from a square box via a hole, we introduce the probabilities $P_n(t)$, for which at least n disks remain inside the box at time t ($n = 1, 2, \cdots, N$) [46]. We call this probability $P_n(t)$ "the n-particle survival probability", or simply the survival probability, as a generalization of the well-known survival probability discussed in one-particle escape systems [30, 34, 35]. For almost arbitrary initial conditions, except for some specific cases, for example, that disks move in a periodic orbit without reaching the hole, the n-particle survival probability goes to zero, i.e. $\lim_{t\to+\infty} P_n(t) = 0$, in the long time limit $t \to +\infty$, and escape properties of many-particle systems are characterized by decay properties of $P_n(t)$.

In Fig. 2 we show graphs of the n-particle survival probabilities $P_n(t)$ of N hard disks as functions of time t for $n = 5$ (the solid line), 4 (the dashed line), 3 (the dotted line), 2 (the dash-dotted line), 1 (the dash-double-dotted line) with $N = 5$. Here, we used values of the parameters as $m = 1$, $r = 1/2$, $h = 0.1(L - 2r)$ and $\rho = 0.1$ (so $L \approx 6.27$). For the survival probabilities shown in Fig. 2, we calculated 5×10^8 number of ensembles from random initial conditions at $t = 0$ in which the disk positions and momenta are distributed into the microcanonical distribution of the system without the hole with the value N of energy E [47, 48].

The main figure of Fig. 2 is the log-log plots of the n-particle survival probabilities $P_n(t)$, $n = 1, 2, \cdots, 5$. As shown clearly as a straight line in this figure, the 1-particle survival probability $P_1(t)$ decays in power after

a long time. We fitted this power decay of $P_1(t)$ to a power function $\alpha_1 t^{-1}$ with the value $\alpha_1 = 86.6$ of the fitting parameter α_1. This result is simply explained by the fact that only a single disk exists in the majority of times in the decay of $P_1(t)$ and a single disk in the square box is not chaotic, leading to the power decay $\sim t^{-1}$ of the survival probability [30]. On the other hand, as shown in the inset of Fig. 2 as linear-log plots of $P_n(t)$, the N-particle survival probability $P_N(t)$ decays exponentially in time. To clarify this property, we fitted the graph of $P_N(t)$ to an exponential function $\exp(-\alpha_2 t)$ with the value $\alpha_2 = 3.65 \times 10^{-2}$ of the fitting parameter α_2, which is almost indistinguishable with the graph of $P_N(t)$ in the inset of Fig. 2. It should be noted that an exponential decay of the survival probability also appears in one-particle chaotic systems [30].

C. Exponential decays of survival probabilities

Now, we proceed to discuss decay properties of the n-particle survival probabilities $P_n(t)$ for the middle numbers $n = 2, 3, \cdots, N-1$. The inset of Fig. 2 suggests that different from the graph of $P_N(t)$, the graphs of $P_n(t)$ for $n = 2, 3, \cdots, N-1$ do not seem to show simple exponential decays at early times, although n disks for $n = 2, 3, \cdots, N-1$ can involve disk-disk collisions making the system to be chaotic.

In order to describe decay behaviors of the survival probabilities $P_n(t)$, $n = 2, 3, \cdots, N-1$ at early times, we introduce the probability density $f_k(\tau)$ of the time τ for the k-th disk escape to occur (i.e. the escape time τ of k disks), for $k = 1, 2, \cdots, N$. Using the escape-time probability density $f_k(\tau)$ of k disks, the $(N-k+1)$-particle survival probability $P_{N-k+1}(t)$ for $N-k+1$ disks to remain inside the box at time t is represented as

$$P_{N-k+1}(t) = 1 - \int_0^t d\tau \; f_k(\tau), \tag{1}$$

so that we obtain

$$f_k(\tau) = -\frac{dP_{N-k+1}(\tau)}{d\tau}, \tag{2}$$

$k = 1, 2, \cdots, N$. By Eq. (2), for example, if the N-particle survival probability $P_N(t)$ decays exponential in time, i.e. $P_N(t) = \exp(-at)$ with a positive constant a as shown in Fig. 2, then we obtain the escape-time probability density $f_1(\tau) = \tilde{f}_1(\tau; a)$ for the first escaping disk, in which $\tilde{f}_1(\tau; a)$ is given by

$$\tilde{f}_1(\tau; a) = a e^{-a\tau} \tag{3}$$

for $N > 1$. Equation (1) or (2) also leads to the normalization condition $\int_0^{+\infty} d\tau \; f_k(\tau) = 1$ of the escape-time probability density $f_k(\tau)$ as far as the survival probability $P_{N-k+1}(t)$ goes to zero in the long time limit, i.e. $\lim_{t\to+\infty} P_{N-k+1}(t) = 0$, noting the initial condition $P_{N-k+1}(0) = 1$ of the survival probability.

The escape time τ of k disks is represented as the sum $\tau = \sum_{j=1}^{k} \tau_j$ of the time-interval $\tau_j \equiv t_j - t_{j-1}$ from the time t_{j-1} of the $(j-1)$-th escape to the time t_j of j-th escape of the k disks, defining $t_0 \equiv 0$. For the case that the dynamics of k disks inside the box is chaotic and the probability for each disk to stay inside the box decays exponentially in time, we assume that the probability density of the time τ_k for k-th escaping disk is independent of other times τ_j, $j = k-1, k-2, \cdots, 1$, and the probability density $f_k(\tau)$ of the escape time τ satisfies the recurrence relation $f_k(\tau) = \int_0^\tau ds \; f_1(\tau - s) f_{k-1}(s)$ with $f_1(\tau_k) = \tilde{f}_1(\tau_k; a_k)$ and a positive constant a_k. Under this assumption, we obtain the probability density $f_k(\tau) = \tilde{f}_k(\tau)$ of the escape time τ of the k disks with $k \geq 2$, in which $\tilde{f}_k(\tau)$ is given by

$$\begin{aligned}
\tilde{f}_k(\tau) &= \int_0^\tau dt_k \tilde{f}_1(\tau - t_k; a_k) \int_0^{t_k} dt_{k-1} \tilde{f}_1(t_k - t_{k-1}; a_{k-1}) \\
&\quad \times \int_0^{t_{k-1}} dt_{k-2} \tilde{f}_1(t_{k-1} - t_{k-2}; a_{k-2}) \cdots \int_0^{t_3} dt_2 \tilde{f}_1(t_3 - t_2; a_2) \tilde{f}_1(t_2; a_1) \qquad (4) \\
&= \left(\prod_{j=1}^{k} a_j \right) \sum_{j=1}^{k} \frac{e^{-a_j \tau}}{(a_1 - a_j)(a_2 - a_j) \cdots (a_{j-1} - a_j)(a_{j+1} - a_j)(a_{j+2} - a_j) \cdots (a_k - a_j)}, \qquad (5)
\end{aligned}$$

in which we assumed the condition $a_j \neq a_k$ for $j \neq k$. From Eqs. (1) and (5) we derive the $(N-k+1)$-particle survival probability $P_{N-k+1}(t) = \tilde{P}_{N-k+1}(t)$, in which $\tilde{P}_{N-k+1}(t)$ is given by

$$\tilde{P}_{N-k+1}(t) = \sum_{j=1}^{k} \frac{a_1 a_2 \cdots a_{j-1} a_{j+1} a_{j+2} \cdots a_k e^{-a_j t}}{(a_1 - a_j)(a_2 - a_j) \cdots (a_{j-1} - a_j)(a_{j+1} - a_j)(a_{j+2} - a_j) \cdots (a_k - a_j)} \tag{6}$$

for $k = 2, \cdots, N-1$. The derivation of Eq. (5) from Eqs. (3) and (4), as well as the derivation of Eq. (6) from Eqs.

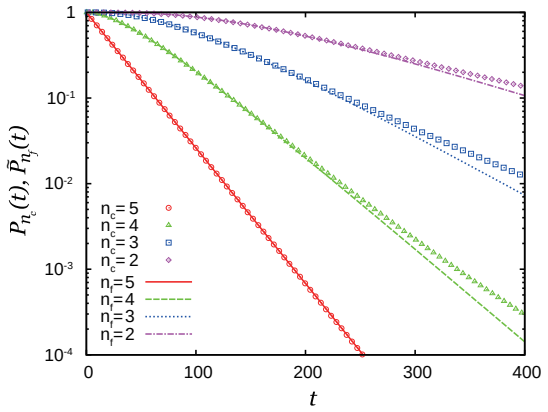

FIG. 3: (Color online) Fittings of the n-particle survival probabilities $P_n(t)$ of a 5-disk system to the functions $\tilde{P}_n(t)$ as functions of time t for $n = 5, 4, 3, 2$ with the the fitting parameters a_j, $j = 1, 2, 3, 4$, on linear-log plots. Here, $P_n(t)$ and $\tilde{P}_n(t)$ are shown as the open circles and the solid line for $n = 5$, the triangles and the broken line for $n = 4$, the squares and the dotted line for $n = 3$, and the diamonds and the dash-dotted line for $n = 2$, respectively.

(1) and (5), are given in Appendix A. Here, the 1-particle survival probability $P_1(t)$ would not be justified by Eq. (6), because the dynamics of the last single disk inside the box is not chaotic.

In Fig. 3 we show fittings of the n-particle survival probabilities $P_n(t)$ for $n = 5$ (the circles), 4 (the triangles), 3 (the squares) and 2 (the diamonds) to the functions $\tilde{P}_n(t)$ for $n = 5$ (the solid line), 4 (the broken line), 3 (the dotted line), 2 (the dash-dotted line), respectively, with fitting parameters a_j, $j = 1, 2, \cdots, 4$. Here, the n-particle survival probabilities $P_n(t)$ in this figure is the same as those in Fig. 2, and we defined the function $\tilde{P}_N(t)$ by $\tilde{P}_N(t) \equiv \exp(-a_1 t)$, while the function $\tilde{P}_n(t)$, $n = 2, \cdots, N-1$ are given by Eq. (6). In these fittings, we first fitted the N-particle survival probability $P_N(t)$ to $\tilde{P}_N(t)$ with a fitting parameters a_1, then fitted the $(N-j+1)$-particle survival probability $P_{N-j+1}(t)$ to $\tilde{P}_{N-j+1}(t)$ with a fitting parameters a_j and the already fitted values of $a_1, a_2, \cdots, a_{j-1}$, for $j = 2, 3, \cdots, N-1$. The concrete values of the fitting parameters a_j, $j = 1, 2, \cdots, 4$ used for the functions $\tilde{P}_n(t)$ in Fig. 3 are shown as the data for $\rho = 0.1$ and $h/(L-2r) = 0.1$ in Table I. As shown in Fig. 3, the function (6) fits the n-particle survival probability $P_n(t)$ reasonably well at early times for $n = 2, 3, \cdots, N-1$.

In Table I we show the fitting values of the exponential decay rates a_j, $j = 1, 2, 3, 4$, divided by the quantity $\tilde{a} \equiv hv_0/(L-2r)^2$ with the one-particle initial average speed $v_0 \equiv \sqrt{2mE/N}$, for various initial particle densities ρ and ratios $h/(L-2r)$ of the hole size h to the effective side length $L-2r$ of the box, in the survival probabilities $P_n(t)$, $n = 1, 2, 3, 4$ of 5-disk systems at early times. Here, the system parameters used

ρ	$L-2r$	$h/(L-2r)$	$\tilde{a}$	$a_1/\tilde{a}$	$a_2/\tilde{a}$	$a_3/\tilde{a}$	$a_4/\tilde{a}$
10^{-1}	5.27	10^{-1}	2.69×10^{-2}	1.36	0.933	0.607	0.358
10^{-2}	18.8	10^{-1}	7.52×10^{-3}	1.08	0.802	0.565	0.357
10^{-3}	61.7	10^{-1}	2.29×10^{-3}	1.08	0.806	0.578	0.355
10^{-1}	5.27	10^{-2}	2.69×10^{-3}	1.37	0.952	0.632	0.369
10^{-1}	5.27	10^{-3}	2.69×10^{-4}	1.38	0.956	0.640	0.372

TABLE I: Decay rates a_n, $n = 1, 2, 3, 4$, divided by $\tilde{a} \equiv hv_0/(L-2r)^2$, for a 5-disk system with various values of the initial particle density ρ and the hole size ratio $h/(L-2r)$.

to obtain these data, other than those shown in Table I and the ensemble number 2×10^8 only for the case of $(\rho, h/(L-2r)) = (10^{-1}, 10^{-3})$, are the same as those of the system whose survival probabilities are shown in Fig. 2. The factor $1/\tilde{a}$ used for the quantities $a_j/\tilde{a}$ in this table, comes from the fact that the exponential decay rate of the survival probability in escapes of a single chaotic point particle via a small hole in a two-dimensional space is proportional to $hv_0/\mathcal{S}$ with the hole size h, the particle speed v_0, and the area $\mathcal{S}$ for the point particle to move before escaping [30]. Table I suggests that the quantity $a_j/\tilde{a}$ for each value of j takes similar values for a wide variety of initial particle densities ρ and hole size ratios $h/(L-2r)$ like in escapes of a single particle, although the value of $a_j/\tilde{a}$ decreases as the index j increases.

D. Disk-disk collisions and power decays of survival probabilities

Now we proceed to discuss the effects of disk-disk collisions in decays of the n-particle survival probability $P_n(t)$ after a long time.

For comparisons in the discussions on effects of disk-disk collisions, we calculate survival probabilities of another type of many-disk systems in which disks can overlaps with each other. (This type of disk systems without any disk-disk collision may be regarded as the ones consisting of N point-particles in the square box which has the side length $L-2r$ and the hole in the region of the length r in both the sides from a single corner of the box.) Figure 4 is the graphs of the n-particle survival probabilities $P'_{n_0}(t)$ of such 5 disks without their collisions for $n_0 = 5$ (the solid line), 4 (the dashed line), 3 (the dotted line), 2 (the dash-dotted line) and 1 (the dash-double-dotted line), as well as the n-particle survival probabilities $P_{n_c}(t)$ of 5 disks with their collisions for $n_c = 5$ (the circles), 4 (the triangles), 3 (the squares), 2 (the diamonds) and 1 (the inverted triangles). Here, the survival probabilities $P_{n_c}(t)$ are the same as in Fig. 2, and all values of the system parameters for the survival probabilities $P'_{n_0}(t)$ are the same as those for $P_{n_c}(t)$ except for the conditions in which disks can overlap without any impact in their time-evolutions and the initial velocity distribution of each particle is given by a uni-

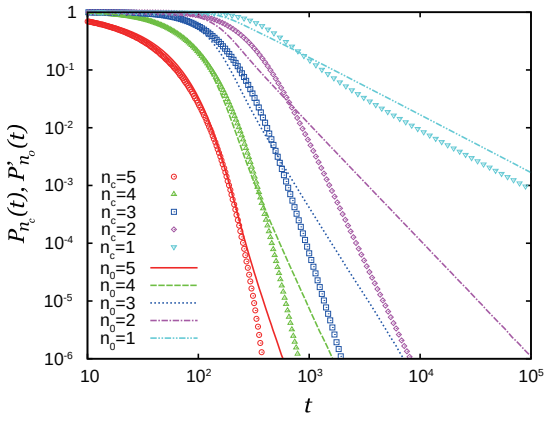

FIG. 4: (Color online) The n_0-particle survival probabilities $P'_{n_0}(t)$ of a 5-disk system without any disk-disk collision as functions of time t for $n_0 = 5$ (the solid line), 4 (the dashed line), 3 (the dotted line), 2 (the dash-dotted line) and 1 (the dash-double-dotted line), and the n_c-particle survival probability $P_{n_c}(t)$ of a 5-disk system with disk-disk collisions as functions of time t for $n_c = 5$ (the circles), 4 (the triangles), 3 (the squares), 2 (the diamonds) and 1 (the inverted triangles), on log-log plots.

form distribution under the constraint for the speed of each particle to be 1, imposing the microcanonical distribution for each independent particle at the initial time $t = 0$.

It is shown in Fig. 4 that at some early times the survival probabilities $P'_{n_0}(t)$, $n_0 = 4, 3, \cdots, 1$ of the system without any disk-disk collision decay faster than the corresponding survival probabilities $P_{n_c}(t)$, $n_c = 4, 3, \cdots, 1$ of the system with disk-disk collisions. In contrast, after a long time the survival probabilities $P'_{n_0}(t)$ decay slower than the corresponding survival probabilities $P_{n_c}(t)$. We can also recognize in Fig. 4 that after a long time the survival probabilities $P'_1(t)$ decays in power $\sim t^{-1}$, similar to the survival probability $P_1(t)$.

It is important to note in Fig. 4 that unlike the survival probability $P_1(t)$, decays of the survival probabilities $P_{n_c}(t)$, $n_c = 2, 3, \cdots, N-1$ show essential differences from those of the corresponding survival probabilities $P'_{n_0}(t)$, $n_0 = 2, 3, \cdots, N-1$ after a long time. However, it is rather unclear to discuss power decays of these survival probabilities $P_{n_c}(t)$ after a long time by their fittings to power functions in Fig. 4. To clarify this point quantitatively, we introduce the function $F_n(t)$ defined by

$$F_n(t) \equiv \frac{d \ln P_n(t)}{d \ln t} = \frac{t}{P_n(t)} \frac{dP_n(t)}{dt}, \tag{7}$$

which takes a constant value if the n-particle survival probability $P_n(t)$ decays in power [49]. (It may be noted that if the survival probability $P_n(t)$ decays exponentially in time as $P_n(t) = \exp(-at)$ with a positive constant a, then the function (7) becomes $-at$, leading to the initial

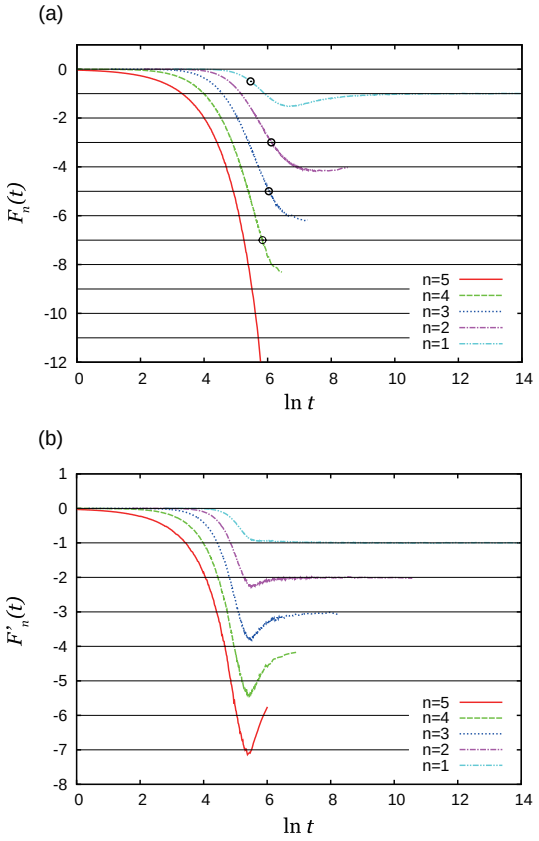

FIG. 5: (Color online) (a) The slops $F_n(t)$ of the quantities $\ln P_n(t)$, and (b) the slops $F'_n(t)$ of the quantities $\ln P'_n(t)$, as functions of $\ln t$ for $n = 5$ (the solid line), 4 (the dashed line), 3 (the dotted line), 2 (the dash-dotted line) and 1 (the dash-double-dotted line) for 5-disk systems. The open circles in (a) are the points for the slop $F_n(t)$ to cross the line $-(2n-1)$ for $n = 4, 3$ and 2 and the line $-1/2$ for $n = 1$.

value $F_n(0) = 0$ of the function $F_n(t)$.) In Fig. 5(a) we show the slops $F_n(t)$ of $\ln P_n(t)$ as functions of $\ln t$ for $n = 5$ (the solid line), 4 (the dashed line), 3 (the dotted line), 2 (the dash-dotted line) and 1 (the dash-double-dotted line), for the 5-disk system with disk-disk collisions. For a comparison, in Fig. 5(b) we also show the slops $F'_n(t) \equiv d \ln P'_n(t)/d \ln t$ of $\ln P'_n(t)$ as functions of $\ln t$ for $n = 5$ (the solid line), 4 (the dashed line), 3 (the dotted line), 2 (the dash-dotted line) and 1 (the dash-double-dotted line), for the corresponding 5-disk system without any disk-disk collision. Here, we used the systems whose n-particle survival probabilities $P_n(t)$ and $P'_n(t)$ are shown in Fig. 4.

Figure 5 shows that both the 1-particle survival probabilities $P_1(t)$ and $P'_1(t)$ decay in power $\sim t^{-1}$ after a long time, but power decay properties of other n-particle survival probabilities $P_n(t)$ and $P'_n(t)$ for $n = 2, 3, \cdots, N-1$ after a long time are different with each other. For the case with disk-disk collisions, Fig. 5(a) shows that the survival probabilities $P_2(t)$ and $P_3(t)$ decay in power

$\sim t^{-4}$ and $\sim t^{-6}$, respectively, suggesting their asymptotic power decays as

$$P_n(t) \overset{t\to+\infty}{\sim} \begin{cases} \eta_1 t^{-1} & \text{for } n=1 \\ \eta_n t^{-2n} & \text{for } n=2,3,\cdots, \end{cases} \tag{8}$$

with constants η_n, $n=1,2,\cdots$, although the graph of $F_4(t)$ in Fig. 5(a) does not show clearly such an asymptotic power decay of the survival probability $P_4(t)$ yet. In contrast, for the case without any disk-disk collision, Fig. 5(b) shows that the survival probabilities $P'_2(t)$, $P'_3(t)$ and $P'_4(t)$ decays in power $\sim t^{-2}$, $\sim t^{-3}$ and $\sim t^{-4}$, respectively, suggesting their asymptotic decays as

$$P'_n(t) \overset{t\to+\infty}{\sim} \eta'_n t^{-n} \quad \text{for } n=1,2,\cdots, \tag{9}$$

with constants η'_n, $n=1,2,\cdots$. The difference between Eqs. (8) and (9) would be regarded as an important effect of disk-disk collisions in decays of the n-particle survival probabilities.

III. FINITE-TIME LYAPUNOV EXPONENTS OF ESCAPE SYSTEMS

A. Decays of finite-time Lyapunov exponents

The system considered in this paper is chaotic, as far as two colliding hard disks exist inside the box. In order to characterize chaotic dynamics of the system with a dynamical instability, we introduce the finite-time largest Lyapunov exponent (FTLLE) $\lambda(t)$ at time t, which is defined by

$$\lambda(t) = \lim_{|\delta\boldsymbol{\Gamma}(0)|\to 0} \frac{1}{t} \ln \frac{|\delta\boldsymbol{\Gamma}(t)|}{|\delta\boldsymbol{\Gamma}(0)|}. \tag{10}$$

Here, $\delta\boldsymbol{\Gamma}(t)$ is a small deviation of the phase space vector (consisting of the position vector and the momentum vector) of the hard disks existing inside the box at time t, and the dimension of the vector $\delta\boldsymbol{\Gamma}(t)$ reduces by four at every time when a disk escapes from the hole. The well-known largest Lyapunov exponent of the system in the non-escape case with $h=0$ is given by $\lim_{t\to+\infty}\lambda(t)$. On the other hand, in the case for disks to escape with $h>0$, even if the system is chaotic initially, then we have $\lim_{t\to+\infty}\lambda(t)=0$ for almost any initial condition for which no disk (or only one disk) exists inside the box in the long time limit $t\to+\infty$. Therefore, we characterize chaotic or non-chaotic properties of the system by a decay behavior of the FTLLE $\lambda(t)$ at time t.

In Fig. 6 we show an example of time-dependences of the FTLLE $\lambda(t)$ as circles, as well as the times t_n for the n-th escape of disks from the box as a vertical line ($n=1,2,\cdots,5$). Here, we used the 5-disk system whose n-particle survival probabilities $P_n(t)$ are shown in Fig. 2. As expected in escape systems, the FTLLE $\lambda(t)$ decays globally, although it can increase temporally by disk-disk collisions. It is important to note for contents of this paper that some local decays of $\lambda(t)$ looks like a straight line in Fig. 6 as a log-log plot of $\lambda(t)$ as a function of t. To specify this property quantitatively, we fitted the FTLLE $\lambda(t)$ in the time period $(300,t_1]$ after the $(N-1)$-th disk escapes at the time $t=t_2$ (<300) until the N-th (i.e. the last) disk escapes at the time $t=t_1$, to a power function $\beta_1 t^{-\beta_2}$ with fitting parameters β_1 and β_2, as shown the straight shin line in Fig. 6. Here, we used the values $\beta_1=128$ and $\beta_2=0.981$ for these fitting parameters. In this time period, there is only one disk inside the box with no disk-disk collision and the system is not chaotic, so this result suggests that the FTLLE decays almost in power $\sim t^{-1}$ after a long time for non-chaotic cases, while the FTLLE should approach to a nonzero finite value for chaotic cases with disk-disk collisions.

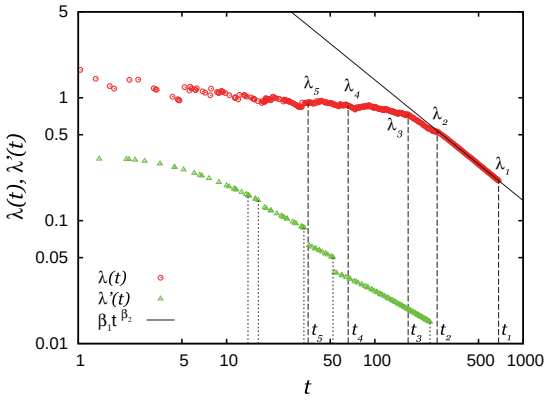

FIG. 6: (Color online) A finite-time largest Lyapunov exponent (FTLLE) $\lambda(t)$ (circles) [$\lambda'(t)$ (triangles)] of a 5-disk system with disk-disk collisions [without any disk-disk collision] as a function of time t on log-log plots. Here, the vertical broken [dotted] lines indicate the times t_n when the n-th escape of the disks from the box occurs with the value λ_n of FTLLE ($n=1,2,\cdots,5$). (In this figure, the symbols t_n and λ_n, $n=1,2,\cdots,5$ are explicitly shown only for the FTLLE $\lambda(t)$.) The straight shin line is a fit to the FTLLE $\lambda(t)$ in the time period $(300,t_1]$ by the power function $\lambda(t)=\beta_1 t^{-\beta_2}$ with the fitting parameters $\beta_j, j=1,2$.

For a comparison, we also show in Fig. 6 an example of time-dependences of the FTLLE $\lambda'(t)$ of the system without any disk-disk collision as triangles. Here, for the calculation of the FTLLE $\lambda'(t)$ we used the same values of system parameters and the initial distribution of $\delta\Gamma(0)$ as those for the FTLLE $\lambda(t)$ in Fig. 6 except for absence of the disk-disk collision, and for the FTLLE $\lambda'(t)$ the initial distribution of $\Gamma(0)$ is taken as same as the system whose n-particle survival probabilities $P'_{n_0}(t)$ are shown in Fig. (4). Different from the FTLLE $\lambda(t)$ for the system with disk-disk collisions, the FTLLE $\lambda'(t)$ in this figure shows a smoothly decreasing function of time, except for some abrupt changes of $\lambda'(t)$ at the escape times of disks.

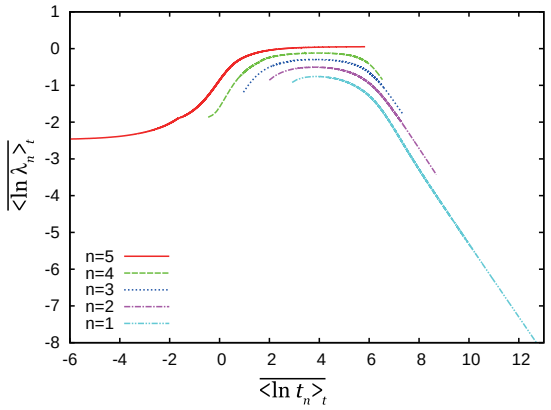

FIG. 7: (Color online) The local time averages $\overline{\langle \ln \lambda_n \rangle_t}$ of $\ln \lambda_n$ as functions of local time averages $\overline{\langle \ln t_n \rangle_t}$ of $\ln t_n$, for $n = 5$ (the solid line), 4 (the dashed line), 3 (the dotted line), 2 (the dash-dotted line) and 1 (the dash-double-dotted line), for a 5-disk system.

B. Averages and fluctuations of the finite-time largest Lyapunov exponents at escape times

Noting that FTLLEs depend on the initial conditions of the phase space vector $\boldsymbol{\Gamma}(t)$ and its deviation $\delta\boldsymbol{\Gamma}(t)$ at the time $t = 0$, we discuss decay properties of FTLLEs via an ensemble average over an initial distribution of $\boldsymbol{\Gamma}(t)$ and $\delta\boldsymbol{\Gamma}(t)$. In order to discuss such statistical properties of FTLLEs, we introduce the value λ_n of a FTLLE $\lambda(t)$ at the time $t = t_n$ when the $(N-n+1)$-th particle escape from the box occurs ($n = 1, 2, \cdots, N$), as shown for the FTLLE $\lambda(t)$ in Fig. 6. To calculate them, we use the initial ensemble in which the initial phase space vector $\boldsymbol{\Gamma}(0)$ is distributed into the micro-canonical distribution with a constant energy E, and components of the initial Lyapunov vector $\delta\boldsymbol{\Gamma}(0)$ are chosen as the ones uniformly distributed under the constraint with a constant value of the amplitude $|\delta\boldsymbol{\Gamma}(0)|$. Starting form these initial ensembles of $\lambda(0)$ and $\delta\boldsymbol{\Gamma}(0)$ we calculate distributions of λ_n and t_n, $n = 1, 2, \cdots, N$.

Figure 7 is the graphs of the local time averages $\overline{\langle \ln \lambda_n \rangle_t}$ of $\ln \lambda_n$ as functions of local time averages $\overline{\langle \ln t_n \rangle_t}$ of $\ln t_n$, for $n = 5$ (the solid line), 4 (the dashed line), 3 (the dotted line), 2 (the dash-dotted line) and 1 (the dash-double-dotted line). The system is the same as that whose n-particle survival probabilities were shown in Fig. 2. Here, in order to obtain the smooth numerical data for Fig. 7 related to the FTLLEs λ_n, we used two kinds of local averages $\langle \cdots \rangle_t$ and $\overline{\cdots}$ for $\mathcal{N}_e = 5 \times 10^8$ number of ensembles of $\lambda_n = \lambda_n^{(j)}$ and $t_n = t_n^{(j)}$, $j = 1, 2, \cdots, \mathcal{N}_e$, with $t_n^{(1)} \le t_n^{(2)} \le \cdots \le t_n^{(\mathcal{N}_e)}$. The first average $\langle X(\lambda_n, t_n) \rangle_t$ of a function $X(\lambda_n, t_n)$ of λ_n and t_n means to take the arithmetic means of the data over every $\mathcal{N}_a = 5 \times 10^3$ values from the beginning of the sorted group $\{X(\lambda_n^{(1)}, t_n^{(1)}), X(\lambda_n^{(2)}, t_n^{(2)}), \cdots, X(\lambda_n^{(\mathcal{N}_e)}, t_n^{(\mathcal{N}_e)})\}$, so that we obtain the local averages $X_n^{(k)} \equiv \sum_{j=1+(k-1)\mathcal{N}_a}^{k\mathcal{N}_a} X(\lambda_n, t_n)/\mathcal{N}_a$, $k = 1, 2, \cdots, \mathcal{N}_e/\mathcal{N}_a$. To smooth out a graph of the data $X_n^{(k)}$ without reducing their data points we further take the second local average $\overline{X_n^{(k)}} \equiv \sum_{l=k-\tilde{\mathcal{N}}_k}^{k+\tilde{\mathcal{N}}_k} X_n^{(l)}/(2\tilde{\mathcal{N}}_k + 1)$ with $\tilde{\mathcal{N}}_k = \mathrm{Min}(10^3, (\mathcal{N}_e/\mathcal{N}_a) - k, k - 1)$, $k = 1, 2, \cdots, \mathcal{N}_e/\mathcal{N}_a$. In Fig. 7 we show the graphs of the quantities $\overline{\langle \ln \lambda_n \rangle_t}$ as functions of $\overline{\langle \ln t_n \rangle_t}$, instead of the ones of the quantities $\ln \overline{\langle \lambda_n \rangle_t}$ as functions of $\ln \overline{\langle t_n \rangle_t}$, to discuss the value of power in power decays of the FTLLEs which would be given by the slop of the quantities $\overline{\langle \ln \lambda_n \rangle_t}$ as functions of $\overline{\langle \ln t_n \rangle_t}$.

Figure 7 suggests that a local average of the N-th FTLLE λ_N converges to the largest Lyapunov exponent after a long time without decay, while the other n-th FTLLEs λ_n, $1, 2, \cdots, N-1$ decay in power after some times because there are quite few disk-disk collisions in orbits taking long times up to the $(N-n+1)$-th disk escape from the box, namely almost non-chaotic orbits with zero Lyapunov exponents. Therefore, a transition from chaotic orbits to non-chaotic orbits would be characterized by the time starting a decay of local averages of the FTLLEs.

In order to investigate quantitatively power decays of local averages of the n-th FTLLEs λ_n, $n = 1, 2, \cdots, N-1$ after a long time, we calculate the slop $\overline{G}_n$ of the local averages $\overline{\langle \ln \lambda_n \rangle_t}$ of $\ln \lambda_n$ as functions of the local averages $\overline{\langle \ln t_n \rangle_t}$ of $\ln t_n$. A constant value of the slop $\overline{G}_n$ in time means a power decay $\sim t^{\overline{G}_n}$ of the local average of the n-th FTLLEs λ_n. In Fig. 8(a), we plotted the slops as the local averages $\overline{G}_n$ of $G_n \equiv \left[\overline{\langle \ln \lambda_n \rangle_t}^{(j+1)} - \overline{\langle \ln \lambda_n \rangle_t}^{(j)}\right] \Big/ \left[\overline{\langle \ln t_n \rangle_t}^{(j+1)} - \overline{\langle \ln t_n \rangle_t}^{(j)}\right]$ as a function of local average $\overline{\widetilde{\ln t_n}}$ of $\widetilde{\ln t_n} \equiv \left[\overline{\langle \ln t_n \rangle_t}^{(j+1)} + \overline{\langle \ln t_n \rangle_t}^{(j)}\right] \Big/ 2$, for $n = 5$ (the solid line), 4 (the dashed line), 3 (the dotted line), 2 (the dash-dotted line) and 1 (the dash-double-dotted line), in which $\overline{\langle \ln \lambda_n \rangle_t}^{(j)}$ and its corresponding quantity $\overline{\langle \ln t_n \rangle_t}^{(j)}$, $j = 1, 2, \cdots, \mathcal{N}_e/\mathcal{N}_a$, are the j-th values of $\overline{\langle \ln \lambda_n \rangle_t}$ and $\overline{\langle \ln t_n \rangle_t}$, respectively, with $\overline{\langle \ln t_n \rangle_t}^{(1)} < \overline{\langle \ln t_n \rangle_t}^{(2)} < \cdots < \overline{\langle \ln t_n \rangle_t}^{(\mathcal{N}_e/\mathcal{N}_a)}$. Fig. 8(a) with Fig. 7 suggests that the local averages of the n-th FTLLEs λ_n, $n = 1, 2, 3$ decay asymptotically in a power $\sim t^{-1}$, while the one of the N-th FTLLEs λ_N seems to converge to a positive value as the largest Lyapunov exponent without decaying to zero. For a comparison, in Fig. 8(b) we show the slop $\overline{G'}_n$ for the system without any disk-disk collision, for $n = 5$ (the solid line), 4 (the dashed line), 3 (the dotted line), 2 (the dash-dotted line) and 1 (the dash-double-dotted line). Here, the slop $\overline{G'}_n$ were calculated in the same system and the same calculation process as the one for the slop $\overline{G}_n$ except for an absence of disk-disk collision and the initial distribution of $\Gamma(0)$ used in the system whose n-particle survival probabilities $P'_{n_0}(t)$ are shown in Fig. (4). For the

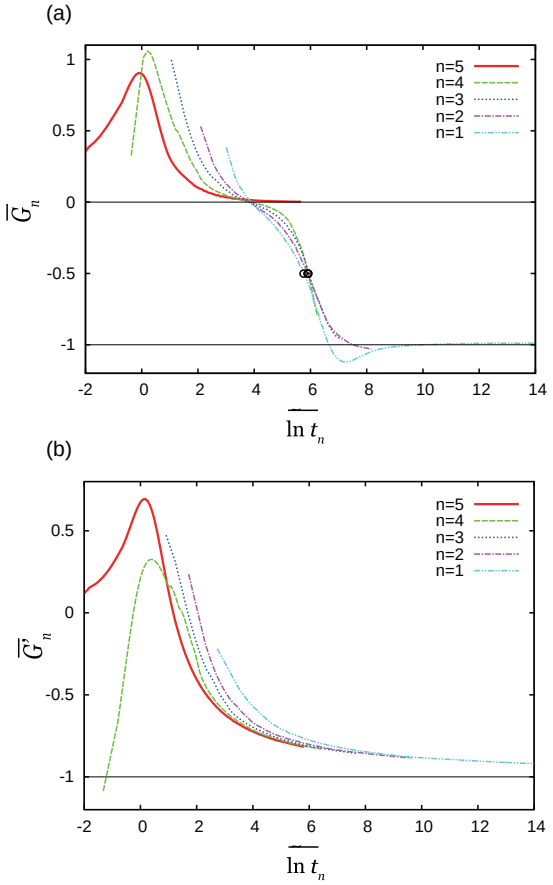

FIG. 8: (Color online) (a) The slops $\overline{G}_n$ [(b) The slops $\overline{G'}_n$] as functions of the local average $\overline{\ln t_n}$ of the logarithm of time t_n, for $n = 5$ (the solid line), 4 (the dashed line), 3 (the dotted line), 2 (the dash-dotted line) and 1 (the dash-double-dotted line), for a 5-disk system with disk-disk collisions [without any disk-disk collision]. The open circles in (a) are the points for the slops $\overline{G}_n$ to have the value -0.5 for $n = 4, 3, 2, 1$.

case without any disk-disk collision, all of the slops $\overline{G'}_n$, $n = 1, 2, \cdots, N$ seem to approach gradually to the value -1 as the time go to infinity. In contrast, the slops $\overline{G}_n$, $n = 1, 2, \cdots, N-1$ for the case with disk-disk collisions, show rapid decays from values around zero to the value -1.

The FTLLEs λ_n, $n = 1, 2, \cdots, N$ as functions of the escape times t_n have large fluctuations, so that it would be meaningful to discuss not only their average properties but also their fluctuations. As a fluctuating feature of the FTLLE λ_n, in Fig. 9 we show the graphs of the averaged ratios $\overline{\langle \Delta\lambda_n^2 \rangle_t / \langle \lambda_n \rangle_t}$ between the local time averages $\langle \Delta\lambda_n^2 \rangle_t$ of the variances $\Delta\lambda_n^2 \equiv (\lambda_n - \langle \lambda_n \rangle_t)^2$ of λ_n and the local time averages $\langle \lambda_n \rangle_t$ of λ_n, as functions of local averages $\overline{\langle t_n \rangle_t}$ of t_n , for $n = 5$ (the solid line), 4 (the dashed line), 3 (the dotted line), 2 (the dash-dotted line) and 1 (the dash-double-dotted line), in the same system as that whose n-particle survival probabilities were shown

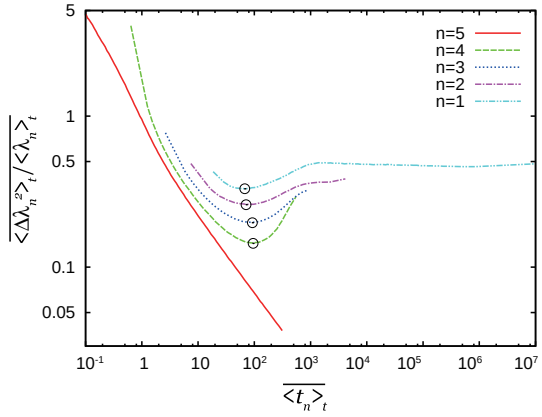

FIG. 9: (Color online) The averaged ratios $\overline{\langle \Delta\lambda_n^2 \rangle_t / \langle \lambda_n \rangle_t}$ as functions of the local averages $\overline{\langle t_n \rangle_t}$ of t_n, for $n = 5$ (the solid line), 4 (the dashed line), 3 (the dotted line), 2 (the dash-dotted line) and 1 (the dash-double-dotted line) for a 5-disk system. The open circles are the points at which the quantities $\overline{\langle \Delta\lambda_n^2 \rangle_t / \langle \lambda_n \rangle_t}$, $n = 4, 3, 2, 1$ take their local minima.

in Fig. 2. This figure shows that a fluctuation amplitude of the N-th FTLLE λ_N continues to decrease as a function of time because the FTLLEs with almost any initial conditions converges to a (positive) Lyapunov exponent as time goes to infinity, known as Oseledec's theorem [50]. In contrast, it is shown in Fig. 9 that variances of the n-th FTLLEs λ_n, divided by the local averages $\langle \lambda_n \rangle_t$ of the FTLLEs λ_n, for $n = 1, 2, \cdots, N-1$ have local minima [the open circles in Fig. 9(b)] as functions of time. After their local minima, the ratios $\overline{\langle \Delta\lambda_n^2 \rangle_t / \langle \lambda_n \rangle_t}$, $n = 1, 2, \cdots, N-1$ increase in time, then seem to reach almost to a constant value as shown for $n = 1, 2$ in Fig. 9, meaning that in this time period variances of the n-th FTLLEs λ_n keep to have a similar amplitude to the local average of the FTLLEs which would go to zero as time goes to infinity. These increases of the quantities $\overline{\langle \Delta\lambda_n^2 \rangle_t / \langle \lambda_n \rangle_t}$ as function of time are supposed to come from non-chaotic orbits which take long times for the $(N - n + 1)$-th disk escape from the box.

C. Relations among transition times in decays of the survival probabilities and the finite-time largest Lyapunov exponents

So far, we have discussed individually decay properties of survival probabilities and FTLLEs of many hard disks in a box with a hole. Now we consider their relations by introducing some times to distinguish those properties of the survival probabilities and the FTLLEs in different time scales.

First, as discussed in Secs. II C and II D, decays of the n-particle survival probabilities $P_n(t)$, $n = 1, 2, \cdots, N-1$ transfer from the superpositions (6) of exponential decays to the power decays (8) for many-hard-disk sys-

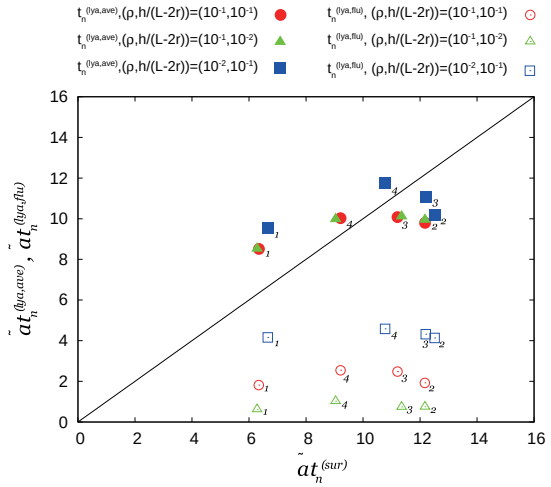

FIG. 10: (Color online) The points $\left(\tilde{a}t_n^{(sur)}, \tilde{a}t_n^{(lya,ave)}\right)$, $n = 2,3,4,5$, for $(\rho, h/(L-2r)) = \left(10^{-1}, 10^{-1}\right)$ (the closed circles), $(\rho, h/(L-2r)) = \left(10^{-1}, 10^{-2}\right)$ (the closed triangles), $(\rho, h/(L-2r)) = \left(10^{-2}, 10^{-1}\right)$ (the closed squares), and the points $\left(\tilde{a}t_n^{(sur)}, \tilde{a}t_n^{(lya,flu)}\right)$, $n = 2,3,4,5$, for $(\rho, h/(L-2r)) = \left(10^{-1}, 10^{-1}\right)$ (the open circles), $(\rho, h/(L-2r)) = \left(10^{-1}, 10^{-2}\right)$ (the open triangles), $(\rho, h/(L-2r)) = \left(10^{-2}, 10^{-1}\right)$ (the open squares) for 5-disk systems. The index number at the right-low side of each point corresponds to the value n of each data for its point. The straight line shows the cases in which $\tilde{a}t_n^{(sur)}$ is equal to $\tilde{a}t_n^{(lya,ave)}$ or $\tilde{a}t_n^{(lya,flu)}$.

tems. As intermediate times for starting their power decays after their decays expressed by the superpositions of exponential decays, we introduce the time $t_n^{(sur)}$, $n = 1,2,\cdots,N-1$ as the times when the slop $F_n(t)$ crosses the line $-1/2$ for $n = 1$ and the line $-(2n-1)$ for $n = 2,3,\cdots,N-1$, respectively. These times are indicated as those of the open circles in Fig. 5(a).

Second, as discussed in Sec III B, the local averages of FTLLEs λ_n at the escape times t_n, $n = 1,2,\cdots,N-1$ decay in power $\sim t^{-1}$ after a long time. These power decays to zero would be caused by non-chaotic orbits of disks which have longer escape times than those of chaotic orbits with frequent disk-disk collisions. We introduce the times $t_n^{(lya,ave)}$, $n = 1,2,\cdots,N-1$ as those for the slops $\overline{G}_n$, $n = 1,2,\cdots,N-1$ to take the value -0.5, respectively, and we use these times to estimate the times after which orbits are almost non-chaotic. The times $t_n^{(lya,ave)}$, $n = 1,2,\cdots,N-1$ are indicated as those of the open circles in Fig. 8(a). Third, we also define the times $t_n^{(lya,flu)}$, $n = 1,2,\cdots,N-1$ as the times when the quantities $\overline{\langle \Delta\lambda_n^2 \rangle_t / \langle \lambda_n \rangle_t}$, $n = 1,2,\cdots,N-1$ take their local minima, respectively, as indicated as the times of the open circles in Fig. 9.

In order to discuss relations among these times $t_n^{(sur)}$, $t_n^{(lya,ave)}$ and $t_n^{(lya,flu)}$, we show in Fig. 10 the points $\left(\tilde{a}t_n^{(sur)}, \tilde{a}t_n^{(lya,ave)}\right)$, $n = 2,3,4,5$, for $(\rho, h/(L-2r)) = \left(10^{-1}, 10^{-1}\right)$ (the closed circles), $(\rho, h/(L-2r)) = \left(10^{-1}, 10^{-2}\right)$ (the closed triangles), $(\rho, h/(L-2r)) = \left(10^{-2}, 10^{-1}\right)$ (the closed squares), and the points $\left(\tilde{a}t_n^{(sur)}, \tilde{a}t_n^{(lya,flu)}\right)$, $n = 2,3,4,5$, for $(\rho, h/(L-2r)) = \left(10^{-1}, 10^{-1}\right)$ (the open circles), $(\rho, h/(L-2r)) = \left(10^{-1}, 10^{-2}\right)$ (the open triangles), $(\rho, h/(L-2r)) = \left(10^{-2}, 10^{-1}\right)$ (the open squares), for the 5-disk systems whose system parameters are the same as the corresponding ones used in Table I. Here, the index number at the right-low side of each point indicates the value n of each data for its point, and the factor $\tilde{a} = hv_0/(L-2r)^2$ is the same as that used in Table I for presenting the exponential decay rates of the survival probabilities for different particle densities ρ and hole size ratios $h/(L-2r)$.

It is important to note in Fig. 10 that the time $t_n^{(sur)}$ takes a quite similar value to the time $t_n^{(lya,ave)}$, $n = 1,2,\cdots,N-1$ for different particle densities ρ and hole size ratios $h/(L-2r)$, noting that the points $\left(\tilde{a}t_n^{(sur)}, \tilde{a}t_n^{(lya,ave)}\right)$ are close on the straight line to indicate the relation $\tilde{a}t_n^{(sur)} = \tilde{a}t_n^{(lya,ave)}$ shown in this figure. This result gives a supportive evidence that a transition from a decay as a superposition (6) of exponential decays to a power decay (8) for the n-particle survival probability $P_n(t)$ corresponds to a transition of the FTLLE λ_n to its power decay caused by non-chaotic properties of the system. It should also be emphasized that the points $\left(t_n^{(sur)}, t_n^{(lya,ave)}\right)$ are well-scaled by multiplying the factor $\tilde{a}$, especially the points $\left(t_n^{(sur)}, t_n^{(lya,ave)}\right)$ for different hole sizes with $h/(L-2r) = 10^{-1}$ and 10^{-2}, shown as almost coincidences of the closed circles and the closed triangles in Fig. 10, reminding the scalings of the decay rates a_j by multiplying by $1/\tilde{a}$ shown in Table I for the exponential decay rates of the survival probabilities. On the other hand, we could not find such kinds of equivalence and scaling between the time $t_n^{(sur)}$ and $t_n^{(lya,flu)}$, although $\tilde{a}t_n^{(sur)}$ and $\tilde{a}t_n^{(lya,flu)}$ have similar orders of magnitudes, as shown in Fig. 10. This figure shows that the quantities $\tilde{a}t_n^{(lya,flu)}$, $n = 1,2,\cdots,N-1$, decrease as the hole size ratio $h/(L-2r)$ decreases, and they increase as the initial particle density ρ decreases.

IV. CONCLUSION AND REMARKS

In this paper, we have discussed escape properties of many hard disks from a square box via a hole. Starting N disks inside the box at the initial time $t = 0$, we introduced the n-particle survival probability as the probability for n ($\leq N$) disks to remain inside the box without escaping up to the time t (≥ 0). Escape behaviors of many hard disks is described qualitatively by

decay properties of the n-particle survival probabilities $P_n(t)$, $n = 1, 2, \cdots, N$, and we showed that at early times the probabilities $P_n(t), n = 2, 3, \cdots, N$ decay as superpositions of exponential functions, while after a long time the probabilities $P_n(t), n = 1, 2, \cdots, N-1$ decay in power. As an important effect of disk-disk collisions, it was shown that the power of the power decay for the probability $P_n(t)(t)$ after a long time is given by $-n$ for $n = 1$ and $-2n$ for $n = 2, 3, \cdots$, in contrast to the case without any disk-disk collision in which the power of the power decay for the n-particle survival probability $P'_n(t)$ after a long time is simply given by $-n$ for $n = 1, 2, \cdots$. This result means that we can obtain informations on the particle number inside the box and particle-particle interactions from decay behaviors of the n-particle survival probabilities. We also discussed scaling properties for exponential decay rates of the probabilities $P_n(t)$ for various hole sizes and initial particle densities.

In order to discuss escape features based on dynamical characteristics of many-particle systems, we introduced the finite time largest Lyapunov exponents (FTLLEs) of hard disks inside a box with a hole. The FTLLE is defined as the exponential rate of expansion or contraction of the absolute magnitude of a small deviation of the phase space vector of the system at a finite time, and it converges to a non-zero finite value as the largest Lyapunov exponent for chaotic system with a dynamical instability in the long time limit. The dynamics of an escape system consisting of many hard disks in a box should be chaotic at early times for disk-disk collisions, but it becomes non-chaotic in the long time limit for only a single (or even zero) disk to exist inside the box after a long time when other disks have already escaped from the box via a hole. In this sense, a transition from a chaotic dynamics to non-chaotic dynamics occurs in escape systems consisting of many hard disks in a box with a hole. In this paper, we discussed this dynamical transition by decay properties of FTLLEs of the escape systems. We introduced the FTLLE λ_n of many-hard-disk system in a box with a hole at the time $t = t_n$ when the $(N-n+1)$-th disk escape occurs. It was shown that a local time average of the FTLLEs λ_n decays in power $\sim t^{-1}$ after a long time, suggesting that the transition from a chaotic dynamics to a non-chaotic dynamics in escape systems could be described by the transition from the value 0 of the slop of a local time average of $\ln \lambda_n$ with respect to a local time average of $\ln t_n$ to its value -1. We estimated this transition time as the time when this slop of the local time average of $\ln \lambda_n$ takes the intermediate value $-1/2$, and showed that this time may be strongly correlated to the transition time for the n-particle survival probability to decay in power. This result would give a quantitative evidence on a connection between the escape features of many-hard-disk systems and their chaotic or non-chaotic dynamical characteristics. It was also shown that these transition times show scaling behaviors on initial particle densities and hole sizes. We also discussed a fluctuation property of the FTLLEs λ_n in the sense that a local time variation of λ_n divided by a local average of λ_n takes a local minimum, then takes a locally almost constant value, as a function of time.

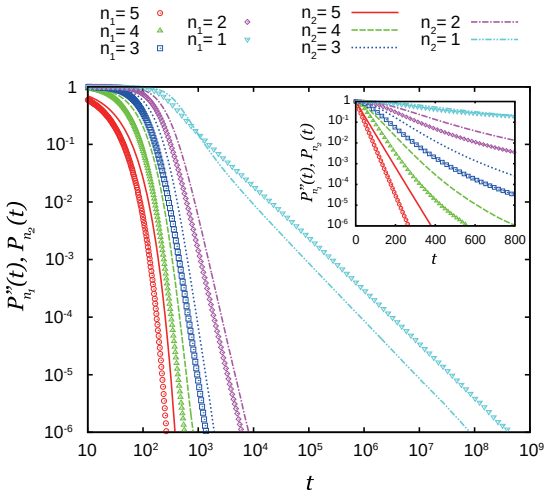

FIG. 11: (Color online) The n_1-particle [n_2-particle] survival probabilities $P''_{n_1}(t)$ [$P_{n_2}(t)$] of a 5-disk system as functions of time t for $n_1 = 5$ (the circles), 4 (the triangles), 3 (the squares), 2 (the diamonds) and 1 (the inverted triangles) [for $n_2 = 5$ (the solid line), 4 (the dashed line), 3 (the dotted line), 2 (the dash-dotted line), 1 (the dash-double-dotted line)] for the hole of the length $r + h$ in a *single side* [for the hole of the length $r + (h/2)$ in *both the sides*] from a single corner of the box. The main figure and the inset are for graphs of $P''_{n_1}(t)$ and $P_{n_2}(t)$ on log-log plots and linear-log plots, respectively.

In the escape model discussed in this paper, we put a single hole for disks to escape, which consists of two regions over *two sides* from a single corner of the box. This hole configuration is chosen so that orbit properties for a disk bouncing between two confronting walls without any collision with other disks, the so-called bouncing ball (or sticky) orbits, is the same for two kinds of the confronting walls. The bouncing ball orbits are known to play an essential role in power decays of survival probabilities in escapes of single-particle billiard models [33, 34]. On the other hand, it would be meaningful to note what happens in particle escapes for different hole configurations. As such an example, in Fig. 11 we show the n_1-particle survival probabilities $P''_{n_1}(t)$ of a 5-disk system as functions of time t for $n_1 = 5$ (the circles), 4 (the triangles), 3 (the squares), 2 (the diamonds) and 1 (the inverted triangles) for the hole of the length $r + h$ in a *single side* from a single corner of the box. Here, except for the hole position we used the same values of the system parameters and the same initial distributions as the system whose survival probabilities are shown in Fig. 2. [In Fig. 11, for comparisons with the survival probabilities $P''_{n_1}(t)$, we also show graphs of the n_2-particle survival probabilities $P_{n_2}(t)$ for $n_2 = 5$ (the solid line), 4 (the dashed line), 3 (the dotted line), 2 (the dash-dotted line), 1 (the dash-double-dotted line), which are the same as in Fig. 2.]

Figure 11 shows that the n-particle survival probabilities $P''_n(t)$ of the escape system with the hole in the single side of the box decay faster than the n-particle survival probabilities $P_n(t)$ of the system with the hole in both the sides of box for $n = 2, 3, \cdots, N$, while the survival probability $P''_1(t)$ decay slower (faster) than the survival probability $P_1(t)$ after a long time (at early times). It should be also noted that the power decay $\sim t^{-1}$ of the survival probability $P''_1(t)$ after a long time looks to be much weaker than that of $P_1(t)$. In general, escape behaviors of disks from the box could depend on where we put a hole, because of not only the properties of periodic orbits but also finite size effects of disks [51]. Another problem involving finite size effects of disks would be an accurate evaluation of decay rates of survival probabilities based on the ergodicity of many-hard-disk systems. Many interesting features including these points, effects of various particle-particle interactions or many holes and so on, would remain as open problems on escape phenomena of many-particle systems.

Appendix A: Derivations of Eqs. (5) and (6)

In this appendix, we derive Eq. (5) from Eqs. (3) and (4), as well as Eq. (6) from Eqs. (1) and (5).

First, we introduce the Laplace transformation $\hat{f}_1(\omega; a) \equiv \int_0^{+\infty} d\tau \ \tilde{f}_1(\tau; a) \exp(-\omega\tau)$ of the function $\tilde{f}_1(\tau; a)$ of τ (> 0), which is given by

$$\hat{f}_1(\omega; a) = \frac{a}{\omega + a} \tag{A1}$$

for $\omega + a > 0$, by using Eq. (3). Second, using Eq. (A1) and the convolution formula of Laplace transformations, the Laplace transformation $\hat{f}_k(\omega) \equiv \int_0^{+\infty} d\tau \ \tilde{f}_k(\tau) \exp(-\omega\tau)$ of the function (4) for $k \geq 2$ is given by

$$\hat{f}_k(\omega) = \prod_{j=1}^{k} \hat{f}_1(\omega; a_j) \tag{A2}$$

$$= \sum_{j=1}^{k} \frac{A_j}{\omega + a_j}. \tag{A3}$$

in a form of the partial fraction under the assumption $a_j \neq a_k$ for $j \neq k$. Here, A_j is a constant and is given by

$$A_j = \lim_{\omega \to -a_j} (\omega + a_j) \sum_{l=1}^{k} \frac{A_l}{\omega + a_l} = \lim_{\omega \to -a_j} (\omega + a_j) \prod_{l=1}^{k} \hat{f}_1(\omega; a_l)$$

$$= \frac{\prod_{l=1}^{k} a_l}{(a_1 - a_j)(a_2 - a_j) \cdots (a_{j-1} - a_j)(a_{j+1} - a_j)(a_{j+2} - a_j) \cdots (a_k - a_j)}. \tag{A4}$$

From Eq. (A3), the inverse-transformation $\tilde{f}_k(\tau)$ of the function $\hat{f}_k(\omega)$ is represented as

$$\tilde{f}_k(\tau) = \sum_{j=1}^{k} A_j e^{-a_j \tau}. \tag{A5}$$

By inserting Eq. (A4) into Eq. (A5), we obtain Eq. (5).

Using Eqs. (A2), (A3) and the normalization condition $\int_0^{+\infty} d\tau \ \tilde{f}_1(\tau; a) = \hat{f}_1(0; a) = 1$ of the probability density $\tilde{f}_1(\tau; a)$, we obtain

$$\int_0^{+\infty} d\tau \ \tilde{f}_k(\tau) = \hat{f}_k(0) = \prod_{j=1}^{k} \hat{f}_1(0; a_j)$$

$$= 1 = \sum_{j=1}^{k} \frac{A_j}{a_j}, \tag{A6}$$

which includes the normalization condition of the probability density $\tilde{f}_k(\tau)$. From Eqs. (1), (A5) and (A6) we derive

$$\tilde{P}_{N-k+1}(t) = 1 - \sum_{j=1}^{k} A_j \frac{1 - e^{-a_j t}}{a_j}$$

$$= \sum_{j=1}^{k} \frac{A_j}{a_j} e^{-a_j t} \tag{A7}$$

for the survival probability $P_{N-k+1}(t) = \tilde{P}_{N-k+1}(t)$ in the case of the probability density $f_k(\tau) = \tilde{f}_k(\tau)$ of the escape time τ of the k disks. By inserting Eq. (A4) into Eq. (A7), we obtain Eq. (6).

[1] G. Gamow, Z. Physik **51**, 204 (1928).

[2] R. W. Gurney and E. U. Condon, Phys. Rev. **33**, 127

(1929).
[3] J. -W. Ryu, S. -Y. Lee, C. -M. Kim, and Y. -J. Park, Phys. Rev. E **73**, 036207 (2006).
[4] S. Shinohara and T. Harayama, Phys. Rev. E **75**, 036216 (2007).
[5] H. J. Kupka, *Transitions in molecular systems* (Wiley-VCH, Weinheim, 2010).
[6] J. Nagler, Phys. Rev. E **69**, 066218 (2004).
[7] J. Binney and S. Tremaine, *Galactic dynamics* (Princeton University Press, Princeton, 2008).
[8] M. Tsuchiya, T. Matsusue, and H. Sakaki, Phys. Rev. Lett. **59**, 2356 (1987).
[9] J. Cooper, C. G. Smith, D. A. Ritchie, E. H. Linfield, Y. Jin, and H. Launois, Physica E **6**, 457 (2000).
[10] S. Miyamoto, K. Nishiguchi, Y. Ono, K. M. Itoh, and A. Fujiwara, Appl. Phys. Lett. **93**, 222103 (2008).
[11] S. R. Wilkinson, C. F. Bharucha, M. C. Fischer, K. W. Madison, P. R. Morrow, Q. Niu, B. Sundaram, and M. G. Raizen, Nature **387**, 575 (1997).
[12] M. C. Fischer, B. Gutiérrez-Medina, and M. G. Raizen, Phys. Rev. Lett. **87**, 040402 (2001).
[13] F. Serwane, G. Zürn, T. Lompe, T. B. Ottenstein, A. N. Wenz, and S. Jochim, Science **332**, 336 (2011).
[14] T. E. Evans, R. A. Moyer, and P. Monat, Phys. Plasmas **9**, 4957 (2002).
[15] R. L. Viana, E. C. Da Silva, T. Kroetz, I. L. Caldas, M. Roberto, and M. A. F. Sanjuán, Phil. Trans. R. Soc. A **369**, 371 (2011).
[16] H. A. Kramers, Physica **7**, 284 (1940).
[17] D. J. Tannor, *Introduction to quantum mechanics; A time-dependent perspective* (University Science Books, 2007).
[18] W. T. Coffey and Y. P. Kalmykov, *The Langevin equation: With applications to stochastic problems in Physics, Chemistry and electrical engineering* (World Scientific, Singapore, 2012).
[19] P. Gaspard and G. Nicolis, Phys. Rev. Lett. **65**, 1693 (1990).
[20] P. Gaspard, *Chaos, scattering and statistical mechanics* (Cambridge University Press, Cambridge, 1998).
[21] R. Klages, *Microscopic chaos, fractals and transport in nonequilibrium statistical mechanics* (World Scientific, Singapore, 2007).
[22] S. Datta, *Electronic transport in mesoscopic systems* (Cambridge University Press, Cambridge, 1995).
[23] Y. Imry, *Introduction to mesoscopic physics* (Oxford University Press, New York, 1997).
[24] J. H. Davies, *The physics of low-dimensional semiconductors* (Cambridge University Press, Cambridge, 1998).
[25] H. Risken, *The Fokker-Planck equation: Methods of solution and applications* (Springer-Verlag, Berlin, 1989).
[26] N. G. van Kampen, *Stochastic processes in physics and chemistry* (Elsevier, Amsterdam, 1992).
[27] E. G. Altmann and T. Tél, Phys. Rev. Lett. **100**, 174101 (2008); Phys. Rev. E **79**, 016204 (2009).
[28] T. Gorin, T. Prosen, T. H. Seligman, and M. Žnidarič, Phys. Rep. **435**, 33 (2006).
[29] Ph. Jacquod and C. Petitjean, Adv. Phys. **58**, 67 (2009).
[30] W. Bauer and G. F. Bertsch, Phys. Rev. Lett. **65**, 2213 (1990); O. Legrand and D. Sornette, Phys. Rev. Lett. **66**, 2172 (1991); W. Bauer and G. F. Bertsch, Phys. Rev. Lett. **66**, 2173 (1991).
[31] I. V. Zozoulenko and T. Blomquist, Phys. Rev. B **67**, 085320 (2003).
[32] L. A. Bunimovich and C. P. Dettmann, Europhys. Lett. **80**, 40001 (2007).
[33] D. N. Armstead, B. R. Hunt, and E. Ott, Physica D **193**, 96 (2004).
[34] C. P. Dettmann and O. Georgiou, Physica D **238**, 2395 (2009).
[35] E. G. Altmann, J. S. E. Portela, and T. Tél, Rev. Mod. Phys. **85**, 869 (2013).
[36] T. Taniguchi and S. Sawada, Phys. Rev. E **83**, 026208 (2011).
[37] T. Taniguchi and S. Sawada, Phys. Rev. A **84**, 062707 (2011).
[38] T. Taniguchi and S. Sawada, Eur. Phys. J. B **86**, 417 (2013).
[39] H. Alt, H. -D. Gräf, H. L. Harney, R. Hofferbert, H. Rehfeld, A. Richter, and P. Schardt, Phys. Rev. E **53**, 2217 (1996).
[40] V. Paar and H. Buljan, Phys. Rev. E **62**, 4869 (2000).
[41] Ch. Dellago, H. A. Posch, and W. G. Hoover, Phys. Rev. E **53**, 1485 (1996).
[42] D. Szász (Ed.), *Hard ball systems and the Lorentz gas* (Springer-Verlag, Berlin, 2000).
[43] T. Taniguchi and G. P. Morriss, Phys. Rev. Lett. **94**, 154101 (2005); Phys. Rev. E **71**, 016218 (2005).
[44] E. Ott, *Chaos in dynamical systems* (Cambridge University Press, Cambridge, 2002).
[45] M. Cencini, F. Cecconi, and A. Vulpiani, *Chaos: From simple models to complex systems* (World Scientific, Singapore, 2010).
[46] In a practical viewpoint, the n-particle survival probability $P_n(t)$ can be calculated as follows. We prepare $\mathcal{M}$ number of initial ensembles of N disks, and for each initial ensemble we calculate the time $t_n^{(j)}$ at which the $(N-n+1)$-th escape of disks via the hole occurs $(j = 1, 2, \cdots, \mathcal{M})$. Then, we take the set of these times with the increasing order as $t_n^{(1)} \le t_n^{(2)} \le \cdots \le t_n^{(\mathcal{M})}$. For the large limit of the ensemble number $\mathcal{M} \to +\infty$, the quantity $\lim_{\mathcal{M}\to+\infty}(\mathcal{M}-j)/\mathcal{M}$ gives the n-particle survival probability $P_n(t)$ at the time $t = t_n^{(j)}$.
[47] E. S. Severin, B. C. Freasier, N. D. Hamer, and D. L. Jolly, Chem. Phys. Lett. **57**, 117 (1978).
[48] R. S. Dumont, J. Chem. Phys. **95**, 9172 (1991).
[49] In a numerical calculation of slop of a function, the numerical data showing the function have to be enough smooth. In the actual numerical calculations of the slops $F_n(t)$ of $\ln P_n(t)$ and $F'_n(t)$ of $\ln P'_n(t)$ shown in Fig. 5 we first took a local time average of $\ln P_n(t)$ and $\ln P'_n(t)$, respectively, then calculated their slops of those locally-smoothed functions.
[50] Ya G. Sinai (Ed.), *Dynamical systems: Collection of papers (Advanced series in nonlinear dynamics, Volume 1)* (World Scientific, Singapore, 1991).
[51] T. Taniguchi and S. Sawada, (unpublished).